Lab Anim Res 2011: 27(2), 153-159
DOI: 10.5625/lar.2011.27.2.153

Laboratory Animal Research
http://submission.kalas.or.kr

Detailed Differentiation of Calbindin D-28k-Immunoreactive Cells in the Dentate Gyrus in C57BL/6 Mice at Early Postnatal Stages

Dae Young Yoo[1†], Ki-Yeon Yoo[2†], Joon Ha Park[3], Ji Won Choi[1], Woosuk Kim[1], In Koo Hwang[1*] and Moo-Ho Won[3*]

[1]*Department of Anatomy and Cell Biology, College of Veterinary Medicine and Research Institute for Veterinary Science, Seoul National University, Seoul, Republic of Korea*
[2]*Department of Oral Anatomy, College of Dentistry, Gangneung-Wonju National University, Gangneung, Republic of Korea*
[3]*Department of Neurobiology, School of Medicine, Kangwon National University, Chuncheon, Republic of Korea*

The hippocampus makes new memories and is involved in mental cognition, and the hippocampal dentate gyrus (DG) is critical because neurogenesis, which occurs throughout life, occurs in the DG. We observed the differentiation of neuroblasts into mature neurons (granule cells) in the DG of C57BL/6 mice at various early postnatal (P) ages: P1, P7, P14, and P21 using doublecortin (DCX) immunohistochemistry (IHC) for neuroblasts and calbindin D-28k (CB) IHC for granule cells. DCX-positive cells decreased in the DG with age; however, CB^+ cells increased over time. At P1, DCX and CB double-labeled (DCX^+CB^+) cells were scattered throughout the DG. At P7, DCX^+CB^+ cells (about 92% of CB^+ cells) were seen only in the granule cell layer (GCL) of the dorsal blade. At P14, DCX^+CB^+ cells (about 66% of CB^+ cells) were found in the lower half of the GCL of both blades. In contrast, at P21, about 18% of CB^+ cells were DCX^+CB^+ cells, and they were mainly located only in the subgranular zone of the DG. These results suggest that the developmental pattern of DCX^+CB^+ cells changes with time in the early postnatal stages.

Keywords: Early postnatal development, subgranular zone, neurogenesis, doublecortin, double immunostaining

Received 18 April 2011; Revised version received 7 June 2011; Accepted 8 June 2011

The hippocampus, which is a part of the limbic system in the brain, makes new memories and is involved in mental cognition [1,2]. In addition, this region is associated with some brain diseases, such as seizures, ischemia, and Alzheimer's disease [3-5]. Recently, this region has been highlighted because neurogenesis occurs in the hippocampal dentate gyrus (DG) throughout life [6-10]. The elimination of granule cells in the DG by neonatal irradiation with X-rays or adrenalectomy in the adulthood results in impaired spatial navigation [11-13].

In the normal development of mice, the peak of granule cell production in the hippocampal DG occurs during the first two weeks of postnatal development [14,15]. Similarly, only 15% of granule cells in the DG are prenatally generated, and an intensive proliferation of these cells occurs during the first postnatal weeks [16].

Many researchers have examined the ontogeny of calbindin D-28k (CB)-containing cells in the DG at early postnatal stages [17-20], and they showed that CB was expressed in granule cells of the DG at very early postnatal stages.

Some markers detect the stages of neurogenesis in the brain. Among these, doublecortin (DCX) expression is thought to be specific for newly generated neurons, since virtually

†These authors contributed equally to this article.

*Corresponding authors: Moo-Ho Won, Department of Neurobiology, School of Medicine, Kangwon National University, 192-1 Hyoja 2-dong, Chuncheon, Gangwon 200-702, Republic of Korea
Tel: +82-33-250-8891; Fax: +82-33-256-1614; E-mail: mhwon@kangwon.ac.kr
In Koo Hwang, Department of Anatomy and Cell Biology, College of Veterinary Medicine, Seoul National University, San 239-1 Daehak-dong, Ganak-gu, Seoul 151-742, Republic of Korea
Tel: +82-2-880-1271; Fax: +82-2-880-1213; E-mail: vetmed2@snu.ac.kr

all DCX-positive cells express early neuronal antigens but lack antigens that are specific to glia, undifferentiated cells, or apoptotic cells [21]. The DCX gene encodes a 40-kDa microtubule-associated protein, which is specifically expressed in neuronal precursors in the developing and adult central nervous system [22]. There are many reports on neural stem cells in the DG using DCX [23-26]. DCX-immunoreactive cells decrease with age after birth.

Although there are studies on the expression of DCX or CB in the postnatal DG, no studies on the detailed development of CB-immunoreactive cells have been combined with DCX. In this study, therefore, we investigated the changes of DCX-immunoreactive neuroblasts and identified the detailed changes of CB-immunoreactive cells using double immunofluorescent staining for DCX and CB in the mouse DG at various early postnatal stages.

Materials and Methods

Experimental animals

We used very young [postnatal day: 1 (P1), 7 (P7), 14 (P14) and 21 (P21), n=12 in each group] male C57BL/6 mice. The day of birth was considered as day 0. Litters were culled to a maximum of eight pups at the day of birth. From any one litter, a maximum of two animals were taken for each age group, ensuring that animals of a given age originated from at least two different litters. The procedures for the handling and care of the animals adhered to the guidelines that comply with the current international laws and policies (NIH Guide for the Care and Use of Laboratory Animals, NIH Publication No. 85-23, 1985, revised 1996) and were approved by the Institutional Animal Care and Use Committee at Hallym's Medical Center (Hallym-1-35). All of the experiments were conducted in a way as to minimize the number of animals used and the suffering caused by the procedures used in the present study.

Tissue processing and cresyl violet staining

The animals at each age were anesthetized by injecting 30 mg/kg Zoletil 50 (Virbac, Carros, France), and the brain was removed. Thereafter, brains were fixed for 24 hours in 4% paraformaldehyde at 4°C and dehydrated with graded concentrations of alcohol before being embedded in paraffin. Thereafter, paraffin-embedded tissues were sectioned on a microtome (Leica Microsystems GmbH, Wetzlar, Germany) into 3-μm coronal sections, and they were mounted onto silane-coated slides. The sections were stained with cresyl violet acetate according to a previously published procedure [3].

Immunohistochemistry (IHC) for DCX and CB

To ensure that the immunohistochemical data were comparable between groups, the sections were carefully processed under the same conditions. The sections were hydrated and treated with 0.3% hydrogen peroxide (H_2O_2) in phosphate-buffered saline (PBS) for 30 min. For antigen retrieval, the sections were placed in 400-mL jars filled with citrate buffer (pH 6.0) and heated in a microwave oven (Optiquick Compact, Moulinex) operating at a frequency of 2.45 GHz and a 800-W power setting. After three heating cycles of 5 min each, slides were allowed to cool at room temperature and were washed in PBS. After washing, the sections were incubated successively in 10% normal rabbit serum in PBS for 30 min and in diluted goat anti-DCX (diluted 1:200, Santa Cruz Biotechnology, Santa Cruz, CA, USA) or rabbit anti-CB (1:5,000, Chemicon International, Temecula, CA, USA) for 48 hours at 4°C. Thereafter, they were exposed to biotinylated rabbit anti-goat IgG or goat anti-rabbit IgG, streptavidin peroxidase complex (diluted 1:200, Vector Laboratories, Burlingame, CA, USA), and then visualized with 3,3-diaminobenzidine tetrahydrochloride (Sigma-Aldrich, St. Louis, MO, USA) in 0.1 M Tris-HCl buffer (pH 7.4).

Double immunofluorescent staining of DCX and CB

In order to confirm the colocalization of DCX and CB in the brain, the sections in the P14 and P21 group were processed by double immunofluorescent staining under the same conditions. Double immunofluorescent staining for goat anti-DCX (diluted 1:25)/rabbit anti-CB (1:500) was performed. The sections were incubated in the mixture of antisera overnight at room temperature. After washing 3 times for 10 min with PBS, they were then incubated in a mixture of both Cy3-conjugated goat anti-rabbit IgG (1:600; Jackson ImmunoResearch Laboratories, West Grove, PA, USA) and FITC-conjugated donkey anti-goat IgG (1:600; Jackson ImmunoResearch Laboratories) for 2 hours at room temperature. The immunoreactions were observed under the AxioM1 microscope-attached HBO100 (Carl Zeiss, Inc., Göttingen, Germany). DCX and CB double-labeled cells in the DG were counted using an image analysis system equipped with a computer-based CCD camera (software: Optimas 6.5, CyberMetrics, Scottsdale, AZ, USA) in 10 sections per animal. Cell counts were obtained by averaging the counts from the sections taken from each animal.

Western blot analysis

In order to confirm the changes in DCX or CB levels in the DG at each age, five animals at each age were sacrificed and used for Western blot analysis. In brief, aliquots containing

20 μg of total protein were boiled in loading buffer containing 150 mM Tris (pH 6.8), 3 mM DTT, 6% SDS, 0.3% bromophenol blue, and 30% glycerol. The aliquots were then loaded onto a 10% polyacrylamide gel. After electrophoresis, the gels were transferred to nitrocellulose transfer membranes (Pall Co., East Hills, NY, USA). To reduce background staining, the membranes were incubated with 5% nonfat dry milk in PBS containing 0.1% Tween 20°C for 45 min, which was followed by incubation with rabbit anti-CB (1:2,000) or goat anti-DCX (1:200), peroxidase-conjugated donkey anti-goat IgG (Sigma-Aldrich) or goat anti-rabbit IgG, and an ECL kit (Pierce, Rockford, IL, USA). The results of the Western blot analysis were scanned, and the quantification of the Western blotting was done using Scion Image software (Scion, Frederick, MD, USA), which was used to measure the optical density. The relative optical density as a percentage of the P1 group is shown in the graph.

Statistical analysis

Data are expressed as mean±SE. The data were evaluated by a one-way ANOVA SPSS program, and the means were assessed using Duncan's multiple-range test in order to elucidate the differences between all age groups. *P*-values <0.05 were considered statistically significant.

Results

Cresyl violet staining

At P1, cells were stained with cresyl violet throughout the DG. Three layers of the DG were not well defined (Figures 1A and 1B). At P7, the DG was divided into three layers: the molecular (ML), the granule cell (GCL), and the polymorphic (PL) layers (Figures 1C and 1D). At P14, the DG was clearly divided into three layers (Figures 1E and 1F). At P21, neuronal cells in all of the layers were clearly stained with cresyl violet (Figures 1G and 1H).

DCX immunoreactivity

At P1, DCX-positive cells were detected in the DG (Figures 2A and 2B), although three layers of the DG were not well defined. At this time, DCX-positive neuroblasts did not have any processes (Figure 2B). DCX-positive neuroblasts were detected in the PL and GCL from P7 (Figures 2C-2H). At P7, DCX-positive neuroblasts had very short processes (Figure 2D). At P14, DCX-positive neuroblasts were also detected in the GCL and PL (Figures 2E and 2F). At this time, DCX-immunoreactive neuroblasts had well-developed processes, which extended into the upper two-thirds of the ML of the DG (Figures 2E and 2F). At P21, DCX-immunoreactive neuroblasts were mainly located in the subgranular zone, as it is named in the adult brain, and the neuroblasts had well-developed processes that extended into the upper two-thirds of the ML (Figures 2G and 2H), although the density and length of the processes were decreased compared to those in the P14 group.

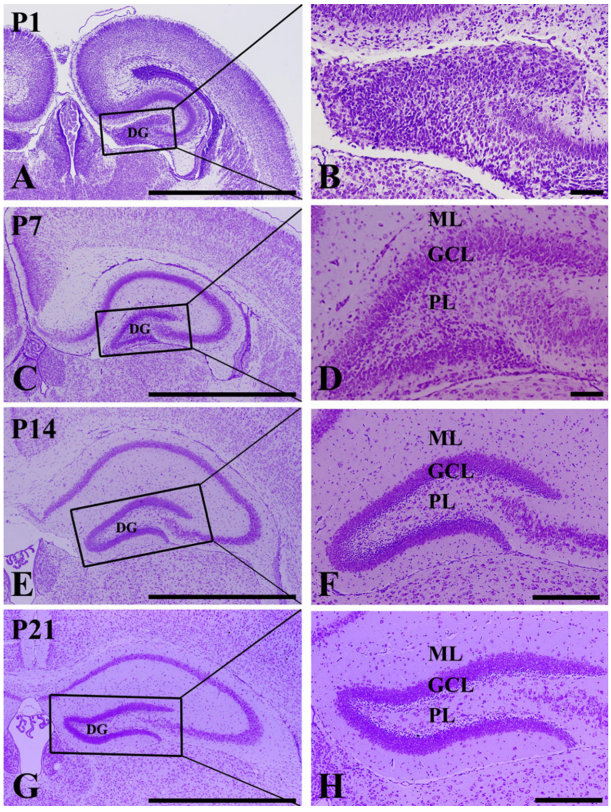

Figure 1. Cresyl violet staining in the mouse dentate gyrus (DG) at postnatal day 1 (P1, A and B), P7 (C and D), P14 (E and F), and P21 (G and H). The DG is well laminated into three layers at P14, and cells in each layer are well distinguished from P14. GCL, granule cell layer; ML, molecular layer; PL, polymorphic layer. Bar=25 μm.

CB immunoreactivity

At P1, CB immunoreactivity was detected in a few neurons that were round in shape in the DG (Figures 3A and 3B). CB immunoreactivity was mainly detected in the GCL and ML from P7 (Figures 3C-3H). At P7, CB-immunoreactive neurons were numerous in the dorsal blade of the GCL; however, CB-immunoreactive neurons in the ventral blade were rarely found (Figures 3C and 3D). In addition, the neuropil of the ML of the dorsal blade was stained with CB immunoreactivity (Figures 3C and 3D). At P14, CB-immunoreactive neurons were distributed in both blades of the GCL, and CB immunoreactivity in the ML was found in both blades (Figures 3E and 3F). At P21, CB immunore-

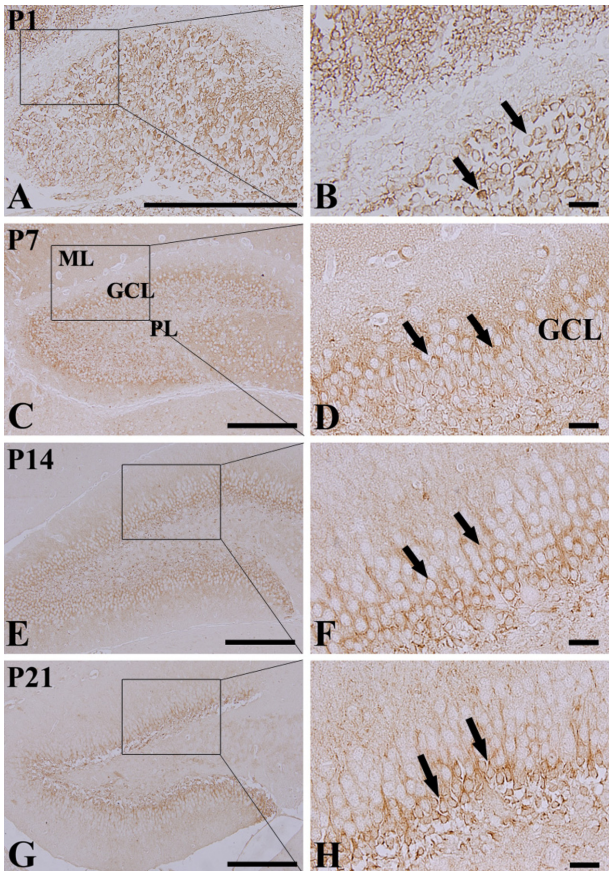

Figure 2. Immunohistochemical staining for doublecortin (DCX) in the DG at P1 (A and B), P7 (C and D), P14 (E and F), and P21 (G and H). At P1, many DCX-positive neuroblasts (arrows) are detected. At P7 and P21, DCX-positive neuroblasts (arrows) are detected in the granule cell layer (GCL). Note that DCX-positive neuroblasts in the GCL are markedly decreased with age, and they are localized at the subgranular zone of the DG. ML, molecular layer; PL, polymorphic layer. Bar=25 μm.

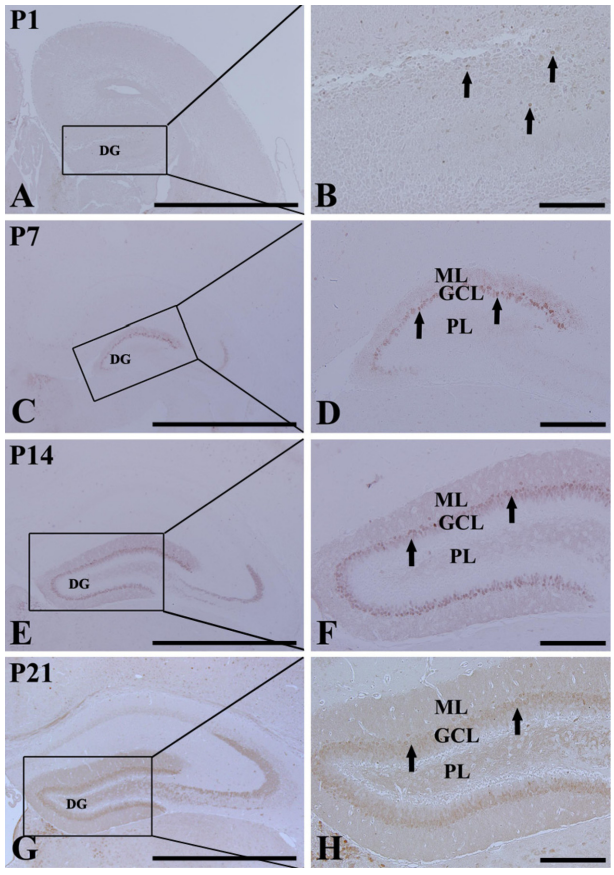

Figure 3. Immunohistochemical staining for calbindin (CB) in the DG at P1 (A and B), P7 (C and D), P14 (E and F), and P21 (G and H). At P1, CB immunoreactivity is detected in a few neurons (arrows). At P7, CB immunoreactivity is mainly detected in the dorsal blade (arrows) of the GCL. CB immunoreactivity is shown in both blades from P14. ML, molecular layer; PL, polymorphic layer. Bar=50 μm.

activity was apparent in granule cells of the GCL and in the neuropil of the ML of both the blades. At this time, the width of the GCL and ML became wider than that at P14 (Figures 3G and 3H).

Colocalization of DCX and CB

At P1, a few DCX and CB double-labeled (DCX^+CB^+) cells were detected throughout the DG (data not shown). At P7, about 92% of CB-positive cells were DCX^+CB^+ cells, and they were distributed throughout the GCL of the dorsal blade only (Figures 4A-4C). At P14, about 66% of CB-positive cells were DCX^+CB^+ cells, and they were found in the lower half of the GCL (Figures 4D-4F). In contrast, at P21, about 18% of the CB-positive cells were DCX^+CB^+ cells, and they were mainly detected only in the subgranular zone of the DG, which is a neurogenic zone in the adult brain (Figures 4G-4I).

DCX and CB protein levels

At P1, DCX protein bands were very strong, and DCX protein levels decreased with age. At P21, DCX protein levels were 47% of that in the P1 group (Figure 5A). At P1, the CB protein bands were very weak, and CB protein levels increased with age. At P21, CB protein levels were 10 times compared to that in the P1 group (Figure 5B).

Discussion

We measured changes in neurons using cresyl violet staining during early postnatal development of C57BL/6 mice in order to demonstrate the maturation of the DG. The layers of the mouse DG were separated into three layers by P14. This is supported by a study that the layers of the DG were separated into three layers by P14 in mice or by P15 in rats [27].

In this study, we observed the distribution pattern of DCX and its protein levels in the DG in order to investigate the

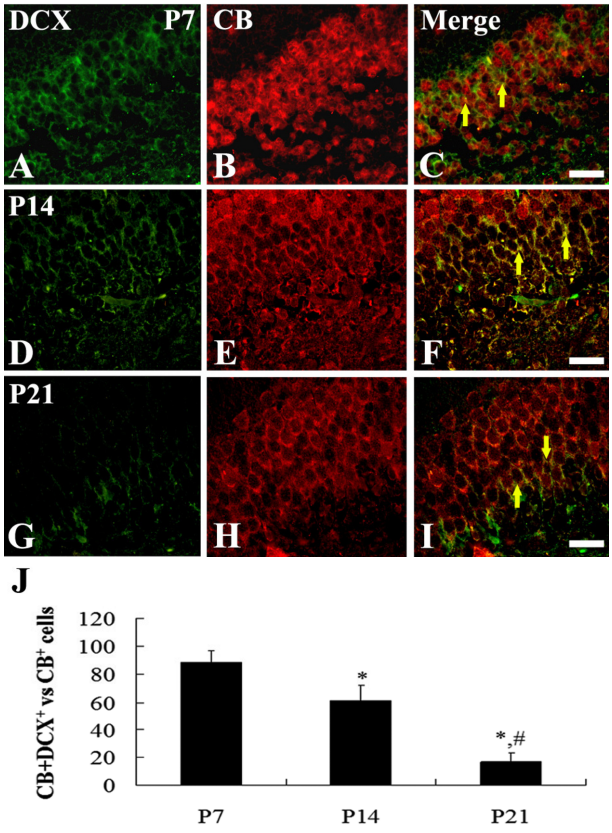

Figure 4. Double immunofluorescent labeling for DCX (A, D and G, green), CB (B, E and H, red), and merged images (C, F and I, yellow) in the DG at P7, P14, and P21. DCX and CB double-labeled (DCX^+CB^+) cells (arrows) are found in the granule cells layer (GCL): Their location is somewhat different from each group. ML, molecular layer; PL, polymorphic layer. Bar=25 μm. J: The mean number of DCX^+CB^+ cells per section (n=7 per group; *P<0.05, significantly different from the P7 group, #P<0.05, significantly different from the P14 group). The bars indicate the means±SE.

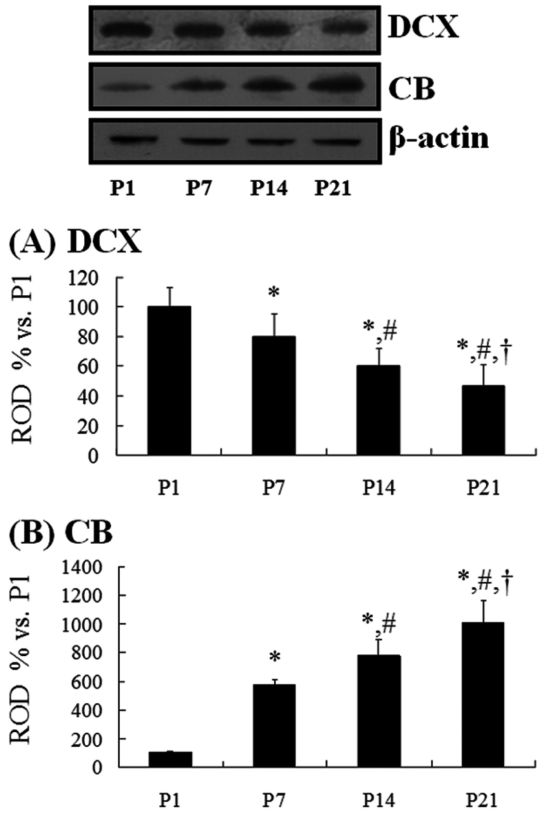

Figure 5. Western blot analyses of DCX (A) and CB (B) in the DG at P1, P7, P14, and P21. The relative optical densities (ROD) of the immunoblot bands are demonstrated as percent values (n=5 per group; *P<0.05, significantly different from the P1 group, #P<0.05, significantly different from the P7 group, †P<0.05, significantly different from the P14 group). The bars indicate the means±SE.

early postnatal changes of neuroblasts in the DG because DCX protein is widely expressed in migrating/differentiating neuroblasts and it is not reexpressed during gliogenesis or regenerative axonal growth [28]. In the present study, we observed that DCX immunoreactivity was selectively located in the periphery of the soma with a pattern that overlapped microtubule distribution [29,30].

At P1, DCX^+ neuroblasts were detected throughout the entire DG. Thereafter, DCX^+ neuroblasts were significantly decreased with time. However, DCX^+ neuroblasts were well developed with time. This result indicates that migrating neuroblasts are significantly decreased in the DG with time at early postnatal stages. It has been reported that postnatally generated neurons are electrically active and capable of firing action potentials and receiving synaptic inputs [31-33], suggesting that they are adequately integrated into existing neuronal circuitry.

CB expression in the GCL of the DG indicates the functional maturity of the hippocampal formation [34,35]. It has been reported that DCX is expressed in the committed progenitor cells and young granule neurons, whereas CB is expressed by mature granule neurons [17]. In addition, it was reported that CB appeared from postnatal day 3 in the granule cells of the rat dentate gyrus and from day 5 in the CA1-CA2 pyramidal cells of Ammon's horn [18]. In the present study, a few CB^+ cells were present at P1, and a general distribution pattern of CB was shown in the dorsal blade of the GCL at P7. We also observed that the majority of CB^+ cells in the GCL was distributed only in the dorsal blade at P7, indicating that the granule cells in the dorsal blade are generated earlier than in the ventral blade. This result is consistent with findings in rats [34] and humans [36]. However, in this study, we used C57BL/6 mice because this is a background strain of many transgenic and knockout mice. In this regard, these basic data could be useful to studies of mutant animals.

In our present study, we observed the coexpression of

DCX^+CB^+ cells in the GCL of the DG. About 92% of CB-positive cells were DCX^+CB^+ cells, which were found only in the dorsal blade. Thereafter, the percentage of DCX^+CB^+ cells vs. CB^+ cells was decreased, and their location in the GCL changed with time. At P21, they were mainly located in the subgranular zone of the DG, which is a neurogenic zone in the adult brain. It has been reported that granule cells start to express CB only at P3-5 [19,34].

However, in order to investigate the role of postnatal neurogenesis in granule cell number control in the rat dentate gyrus, Ciaroni et al. [18] administered methylazoxymethanol, which is a drug that is able to prevent cells from dividing, to the rat on P3, P5, P7, and P9, when the most granule cells are produced. They obtained results that the DG was able to reestablish the proliferative zone and to rebuild the GCL following neonatal methylazoxymethanol administration.

In brief, the lamination in the mouse DG is well defined at P14, and the maturation pattern of granule cells expressing CB in the DG is much changed during very earlier age stages in the C57BL/6 mouse.

Acknowledgments

The authors would like to thank Mr. Seung Uk Lee for his technical help in this study. This study was supported by a 2010 Research Grant from Kangwon National University.

References

1. Fernandes CG, Leipnitz G, Seminotti B, Amaral AU, Zanatta A, Vargas CR, Dutra Filho CS, Wajner M. Experimental evidence that phenylalanine provokes oxidative stress in hippocampus and cerebral cortex of developing rats. Cell Mol Neurobiol 2010; 30(2): 317-326.
2. He WB, Zhang JL, Hu JF, Zhang Y, Machida T, Chen NH. Effects of glucocorticoids on age-related impairments of hippocampal structure and function in mice. Cell Mol Neurobiol 2008; 28(2): 277-291.
3. Hwang IK, Yoo KY, Li H, Park OK, Lee CH, Choi JH, Jeong YG, Lee YL, Kim YM, Kwon YG, Won MH. Indole-3-propionic acid attenuates neuronal damage and oxidative stress in the ischemic hippocampus. J Neurosci Res 2009; 87(9): 2126-2137.
4. Kim Y, Hong S, Noh MR, Kim SY, Huh PW, Park SH, Sun W, Kim H. Inductin of neuron-derived orphan receptor-1 in the dentate gyrus of the hippocampal formation following transient global ischemia in the rat. Mol Cells 2006; 22(1): 8-12.
5. Liu YH, Wang L, Wei LC, Huang YG, Chen LW. Up-regulation of D-serine might induce GABAergic neuronal degeneration in the cerebral cortex and hippocampus in the mouse pilocarpine model of epilepsy. Neurochem Res 2009; 34(7): 1209-1218.
6. Ambrogini P, Cuppini R, Cuppini C, Ciaroni S, Cecchini T, Ferri P, Sartini S, Del Grande P. Spatial learning affects immature granule cell survival in adult rat dentate gyrus. Neurosci Lett 2000; 286(1): 21-24.
7. Ciaroni S, Cecchini T, Ferri P, Ambrogini P, Cuppini R, Lombardelli G, Peruzzi G, Del Grande P. Postnatal development of rat dentate gyrus: effects of methylazoxymethanol administration. Mech Ageing Dev 2002; 123(5): 499-509.
8. Eriksson PS, Perfilieva E, Björk-Eriksson T, Alborn AM, Nordborg C, Peterson DA, Gage FH. Neurogenesis in the adult human hippocampus. Nat Med 1998; 4(11): 1313-1317.
9. Gage FH, Kempermann G, Palmer TD, Peterson DA, Ray J. Multipotent progenitor cells in the adult dentate gyrus. J Neurobiol 1998; 36(2): 249-266.
10. Jaako-Movits K, Zharkovsky T, Pedersen M, Zharkovsky A. Decreased hippocampal neurogenesis following olfactory bulbectomy is reversed by repeated citalopram administration. Cell Mol Neurobiol 2006; 26(7-8): 1559-1570.
11. Conrad CD, Roy EJ. Selective loss of hippocampal granule cells following adrenalectomy: implications for spatial memory. J Neurosci 1993; 13(6): 2582-2590.
12. Czurkó A, Czéh B, Seress L, Nadel L, Bures J. Severe spatial navigation deficit in the Morris water maze after single high dose of neonatal x-ray irradiation in the rat. Proc Natl Acad Sci U S A 1997; 94(6): 2766-2771.
13. Sloviter RS, Sollas AL, Dean E, Neubort S. Adrenalectomy-induced granule cell degeneration in the rat hippocampal dentate gyrus: characterization of an in vivo model of controlled neuronal death. J Comp Neurol 1993; 330(3): 324-336.
14. Bayer SA. Development of the hippocampal region in the rat. II. Morphogenesis during embryonic and early postnatal life. J Comp Neurol 1980; 190(1): 115-134.
15. Schlessinger AR, Cowan WM, Gottlieb DI. An autoradiographic study of the time of origin and the pattern of granule cell migration in the dentate gyrus of the rat. J Comp Neurol 1975; 159(2): 149-175.
16. Altman J, Bayer SA. Postnatal development of the hippocampal dentate gyrus under normal and experimental conditions. In: The Hippocampus (Isaacson RL, Pribram KH, ed), Plenum Press, New York, 1975; pp 95-122.
17. Brandt MD, Jessberger S, Steiner B, Kronenberg G, Reuter K, Bick-Sander A, von der Behrens W, Kempermann G. Transient calretinin expression defines early postmitotic step of neuronal differentiation in adult hippocampal neurogenesis of mice. Mol Cell Neurosci 2003; 24(3): 603-613.
18. Ciaroni S, Cecchini T, Ferri P, Cuppini R, Ambrogini P, Santi S, Benedetti S, Del Grande P, Papa S. Neural precursor proliferation and newborn cell survival in the adult rat dentate gyrus are affected by vitamin E deficiency. Neurosci Res 2002; 44(4): 369-377.
19. Rami A, Bréhier A, Thomasset M, Rabié A. Cholecalcin (28-kDa calcium-binding protein) in the rat hippocampus: development in normal animals and in altered thyroid states. An immunocytochemical study. Dev Biol 1987; 124(1): 228-238.
20. Trejo JL, Cuchillo I, Machin C, Rúa C. Maternal adrenalectomy at the early onset of gestation impairs the postnatal development of the rat hippocampal formation: effects on cell numbers and differentiation, connectivity and calbindin-D28k immunoreactivity. J Neurosci Res 2000; 62(5): 644-667.
21. Rao MS, Shetty AK. Efficacy of doublecortin as a marker to analyse the absolute number and dendritic growth of newly generated neurons in the adult dentate gyrus. Eur J Neurosci 2004; 19(2): 234-246.
22. Jin K, Mao XO, Greenberg DA. Proteomic analysis of neuronal hypoxia in vitro. Neurochem Res 2004; 29(6): 1123-1128.

23. Ganat YM, Silbereis J, Cave C, Ngu H, Anderson GM, Ohkubo Y, Ment LR, Vaccarino FM. Early postnatal astroglial cells produce multilineage precursors and neural stem cells in vivo. J Neurosci 2006; 26(33): 8609-8621.
24. Herrick SP, Waters EM, Drake CT, McEwen BS, Milner TA. Extranuclear estrogen receptor beta immunoreactivity is on doublecortin-containing cells in the adult and neonatal rat dentate gyrus. Brain Res 2006; 1121(1): 46-58.
25. Hwang IK, Yoon YS, Choi JH, Yoo KY, Yi SS, Chung DW, Kim HJ, Kim CS, Do SG, Seong JK, Lee IS, Won MH. Doublecortin-immunoreactive neuronal precursors in the dentate gyrus of spontaneously hypertensive rats at various age stages: comparison with Sprague-Dawley rats. J Vet Med Sci 2008; 70(4): 373-377.
26. Takács J, Zaninetti R, Vig J, Vastagh C, Hámori J. Postnatal expression pattern of doublecortin (DCX) in some areas of the developing brain of mouse. Ideggyogy Sz 2007; 60(3-4): 144-147.
27. Hebel R, Stromberg MW. Anatomy and Embryology of the laboratory rat. In: Nervous system (Hebel R, Stromberg MW, ed), BioMed Verlag, Worthsee, 1986; pp 124-217.
28. Couillard-Despres S, Winner B, Schaubeck S, Aigner R, Vroemen M, Weidner N, Bogdahn U, Winkler J, Kuhn HG, Aigner L. Doublecortin expression levels in adult brain reflect neurogenesis. Eur J Neurosci 2005; 21(1): 1-14.
29. Francis F, Koulakoff A, Boucher D, Chafey P, Schaar B, Vinet MC, Friocourt G, McDonnell N, Reiner O, Kahn A, McConnell SK, Berwald-Netter Y, Denoulet P, Chelly J. Doublecortin is a developmentally regulated, microtubule-associated protein expressed in migrating and differentiating neurons. Neuron 1999; 23(2): 247-256.
30. Gleeson JG, Lin PT, Flanagan LA, Walsh CA. Doublecortin is a microtubule-associated protein and is expressed widely by migrating neurons. Neuron 1999; 23(2): 257-271.
31. Carlén M, Cassidy RM, Brismar H, Smith GA, Enquist LW, Frisén J. Functional integration of adult-born neurons. Curr Biol 2002; 12(7): 606-608.
32. Markakis EA, Gage FH. Adult-generated neurons in the dentate gyrus send axonal projections to field CA3 and are surrounded by synaptic vesicles. J Comp Neurol 1999; 406(4): 449-460.
33. van Praag H, Schinder AF, Christie BR, Toni N, Palmer TD, Gage FH. Functional neurogenesis in the adult hippocampus. Nature 2002; 415(6875): 1030-1034.
34. Abraham H, Orsi G, Seress L. Ontogeny of cocaine- and amphetamine-regulated transcript (CART) peptide and calbindin immunoreactivity in granule cells of the dentate gyrus in the rat. Int J Dev Neurosci 2007; 25(5): 265-274.
35. Molinari S, Battini R, Ferrari S, Pozzi L, Killcross AS, Robbins TW, Jouvenceau A, Billard JM, Dutar P, Lamour Y, Baker WA, Cox H, Emson PC. Deficits in memory and hippocampal long-term potentiation in mice with reduced calbindin D28K expression. Proc Natl Acad Sci U S A 1996; 93(15): 8028-8033.
36. Abrahám H, Veszprémi B, Kravják A, Kovács K, Gömöri E, Seress L. Ontogeny of calbindin immunoreactivity in the human hippocampal formation with a special emphasis on granule cells of the dentate gyrus. Int J Dev Neurosci 2009; 27(2): 115-127.